DJS Vol. 49(1) (2024) – pp.152-171 ISSN: 1012-5965

Delta Journal of Science
Available online at
https://djs.journals.ekb.eg/

Research Article

GEOLOGY

Microstructure and Dielectric Properties of Ceramic Bodies Containing Um Risha Syenite Doped with Coflux Oxides

Salah A. Abead[1*], Ibrahim A. Salem[1], Doaa A. Abdel Aziz[2], Mohamed M. Abu Anbar[1], Mobarak H. Aly[3], Osama M. Hemeda[4] and Basant I. Salem[4]

[1]Geology Department, Faculty of Science. Tanta University, Tanta, Egypt
[2]Ceramic Department, National Research Center, Dokki, Egypt
[3]Environmental Studies and Researcher Institute, University of Sadat City, Sadat City, Egypt
[4]Physics Department, Faculty of Science, Tanta University, Tanta, Egypt

***Corresponding author:** Salah A. Abead **e-mail:** sbmn56@yahoo.com
Received: 26/9/2024 **Accepted:**27/10/2024

KEY WORDS

Um Risha syenite;
physical properties;
ceramic bodies;
microstructure;
Dielectric constant.

ABSTRACT

This paper reported the effect of the addition of Um Risha quartz alkali feldspar syenite from Egypt, which containing a high amount of Fe_2O_3 and alkali oxides mainly K_2O and Na_2O used as a flux material, on the densification properties, sinterability, crystalline phases, microstructure and dielectrical properties of ceramic body composed of 50 Um Risha quartz alkali feldspar syenite, 40 clay and 10 alumina, weight % doped with CuO, MnO_2 and ZnO used as coflux oxides with content 2, 3 and 5 weight %. The physical properties in terms of linear shrinkage, bulk density, water absorption and apparent porosity of the fired ceramic bodies were investigated at different firing temperatures to determine their maturing temperatures. The addition of CuO and MnO_2 reduce the maturing temperature but the addition of ZnO addition has not any effect on the maturing temperature of the fired ceramic bodies. The formed phases in the base sample were quartz, cristobalite, corundum, mullite at 1100 °C. As well as Copper aluminate $CuAl_2O_4$, Manganese aluminate Mn_2AlO_4 and Zinc aluminate $ZnAl_2O_4$ were formed due to the addition of CuO, MnO_2 and ZnO. XRD and SEM analyses were used to examine the development of the phases under consideration. It was observed that the addition of CuO, MnO_2 and ZnO to the base sample increase the dielectric constant, dielectric loss and decrease the resistivity at frequency ranges from 200 Hz to 50 KHz at room temperature.

Introduction

Generally, the ring complexes of Egypt comprise a wide of variety of granites, syenites, gabbros, carbonatites and their volcanic equivalents **El Ramly et al. (1969b, 1970); El Ramly and Hussein, (1982).** Um Risha ring complex area is a part of the Southern Eastern Desert of Egypt. It is located between latitudes 23 ^{o} 15$^{/}$ and 23 ^{o} 20$^{/}$ N and longitudes 33 ^{o} 15$^{/}$ and 33^{o} 20$^{/}$ E (Fig. 1). It is a big structure of magmatic origin representing an area of about 75 Km^2 and is partly covered by Nubian sandstone which break the outcrop into two areas. Um Risha ring complex Composed mainly of alkali feldspar granite and quartz alkali feldspar syenite. Petrographically, the sample for this study is quartz alkali feldspar syenite. It composed mainly of potash feldspar, alkali amphibole, minor alkali pyroxene and minor quartz. The potash feldspar represented mainly by orthoclase, perthite and microcline, whereas the amphibole mainly represented by riebeckite and the alkai pyroxene represented by aegirine.

The most used raw materials in ceramic industries can be basically divided into three main categories: plastic components (clay), fluxing components (feldspars) and filler components (quartz, alumina). Many authors have demonstrated the possibility of a successful substitution of feldspars (flux) by natural resource rocks **Ibrahim et al. (1981); Burat et al. (2006); Ryshchenko et al. (2008); Pantshi and Theart (2008); Salem et al. (2009) and Ismail et al., (2022).**

Fluxes are raw materials with a high amount of alkali oxides, mainly K_2O and Na_2O which reaction with silica and alumina, promote liquid phase formation that facilitates the densification. The liquid phase surrounds the solid particles and by surface tension enables the approach of particles, closing the porosity **Kingery et al. (1975).** The liquid phase fills the original porosity of bodies and promotes densification by viscous flow. Ceramic bodies are manufactured using large amount (40–50 wt %) of fluxes, such as sodic and potassic feldspars, trachytes, nepheline syenite, talc as well as raw materials rich in sodium and potassium oxides. Ceramic bodies with a considerable amount of glassy phase having transition metal ions such as Ni^{2+}, Cu^{2+}, Zn^{2+}, Mn^{2+}, Mn^{3+}, Mn^{4+}, Fe^{3+}, or Cr^{3+} give semiconductor properties **Milankovic et al. (2001) and Abdel Aziz et al. (2010).**

The aim of the present work is to study the effect of the addition of 50 weight % of Um Risha quartz alkali feldspar syenite containing high amount of Fe_2O_3

and alkali oxides mainly K_2O and Na_2O as a flux material on producing ceramic body. Also study the effect of the addition of CuO, MnO_2 and ZnO as coflux oxides on the base composition containing 50 weight% Um Risha quartz alkali feldspar syenite in the presence of clay and alumina to prepare semiconductor ceramic bodies. The prepared ceramic bodies were characterized with respect to the physical, electrical properties and microstructure.

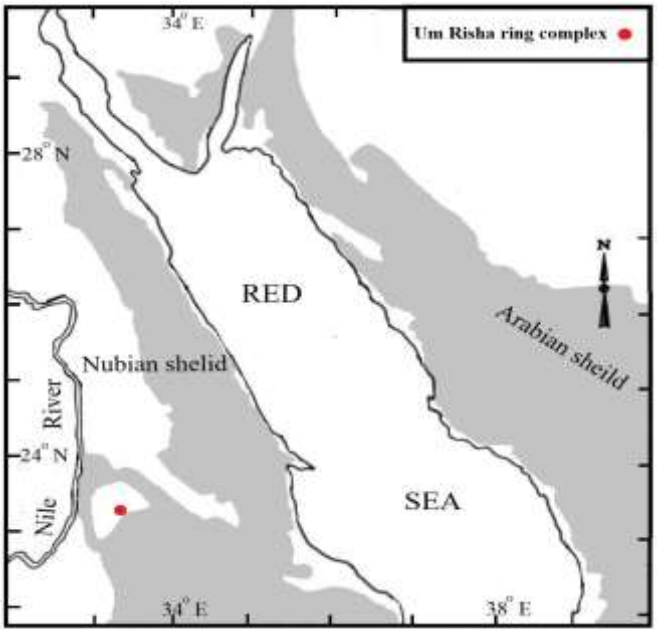

Fig. (1): Map showing the location of Um Risha ring complex, Southern Eastern Desert, Egypt

Experimental work

The starting Egyptian raw materials are Abou Seberia clay from Aswan, Um Risha quartz alkali feldspar syenite from the Southern Eastern Desert of Egypt as a flux material and Aluminum oxide. Finally coflux oxides as CuO (97%), MnO_2 (99.9%) and ZnO (99%) which are used as doping additives. The chemical analyses of the used raw materials are shown in Table (1).

The studied batches are listed in Table (2). The pure base sample (R sample) consisted of 40 Abou Seberia clay, 50 Um Risha quartz alkali feldspar syenite and 10 alumina, weight%. The pure base sample was doped with 2, 3 and 5 weight% CuO, MnO_2 and ZnO that were added above the total ratio weight (100%) of the pure base sample component according to **Abdel Aziz et al. (2010)** as shown in Table (2). The chemical composition of the base sample (R sample) as pure and doped with 2, 3 and 5 weight % CuO, MnO_2 and ZnO are shown in Table (3). The samples were prepared from the fine raw materials which pass through 250 mesh sieve, wet mixed components in ball mill for 2 hrs to attain proper homogeneity, and dried at

110°C by electrical dryer. Discs of 16 mm diameter and ≤ 4.8 mm thickness were processed by semi-dry pressing under a pressure of 230 Kg/cm^2 and dried for 48 h at room temperature, then over night at 110°C in an electrical dryer. The samples were fired between 1000 and 1150°C using fast firing technique, with a temperature interval of about 25 °C/min firing rate, followed by soaking time for 1h, then cooled down to room temperature in a muffle furnace (Carpolite, 20-900522, England).

The physical properties of the fired samples were followed in terms of linear shrinkage, bulk density, apparent porosity and water absorption were determined according to the ASTM specification Nos. C 373-72, C 372-56 and C 326–56 **Anonymons, (1975).** Crystalline phases developed in the vitrified bodies were determined by XRD technique using (X-ray diffractometer by Malvern Panalytical Empyrean device model, (2020) (Netherlands) with Cu-target tube and Ni filter at 40 KV and 30 Ma). Microstructure was studied by scanning electron microscope of the type Environmental Scanning Electron Microscope model Prisma E supported with Ultradry EDS. Operation analytical condition, Low Vacuum with accelerating Volt 30. BSE detector. Electrical properties of the vitrified samples are measured in terms of dielectric constant, dielectric loss and resistivity. The dielectric properties such as capacitance (c) and dissipation factor (tan δ) as well as AC resistance (R) of the prepared samples were measured using RLC Bridge of type BM 591 (Tanta University). The experiments were carried out by applying an electromagnetic field in the frequency value which rises from 200 Hz up to 50 KHz through the prepared ceramic samples at the room temperature. The vitrified samples in the form of discs 15 mm in diameter and ≤ 4.5 mm in thickness were coated with silver paste to ensure a good contact between the sample surfaces and the stainless steel electrodes of the cell capacitor (used for electrical measurements). The dielectric constant (ε′) of the sample is calculated using the relation **(Sindhu et al., 2002)**:

$$(\varepsilon') = 11.3\frac{Cd}{A}$$

The dielectric loss (ε′′) of the sample was measured by the same bridge and calculated using the equation:

$$(\varepsilon'') = \frac{1}{\omega RC} \qquad \omega = 2\pi f$$

f is the frequency in hertz (Hz)

AC electrical resistivity (ρ) (Ω.m) of the samples is calculated using the formula:

$$\rho = \frac{RA}{d}$$

Where C is the measured capacitance of the sample in Pico farad (pF), d is the thickness of the sample in meter (m), A

is the cross-sectional area of the parallel surfaces of the sample in square meter (m^2), R is the AC resistance of the sample in ohm (Ω) and ω is the angular frequency at which the measurements are taken.

Table (1): Chemical analysis of the used raw materials

Oxides %	Um Risha quartz alkali feldspar syenite	Abou Seberia clay	Alumina
SiO_2	65.24	60.78	0.30
Al_2O_3	15.12	26.03	99.7
Fe_2O_3	4.98	1.75	0.02
TiO_2	0.82	1.58	–
CaO	0.93	0.08	–
MgO	0.51	0.26	–
K_2O	4.37	0.55	–
Na_2O	7.06	0.12	0.04
P_2O_5	0.21	0.06	–
MnO	0.26	–	–
SO_3	0.09	0.73	–
L.O.I	0.65	7.88	0.16
Total	100.24	99.82	100.22

Table (2): Batch composition of R sample as pure and doped with 2, 3 and 5 weight % CuO, MnO_2 and ZnO

Batch symbol	Abou Seberia clay	Um Risha quartz alkali feldspar syenite	Alumina	Doping additives		
				CuO	MnO_2	ZnO
R	40	50	10	–	–	–
RCu2	40	50	10	2	–	–
RCu3	40	50	10	3	–	–
RCu5	40	50	10	5	–	–
RMn2	40	50	10	–	2	–
RMn3	40	50	10	–	3	–
RMn5	40	50	10	–	5	–
RZn2	40	50	10	–	–	2
RZn3	40	50	10	–	–	3
RZn5	40	50	10	–	–	5

Table (3): Chemical composition of R sample as pure and doped with 2, 3 and 5 weight % CuO, MnO_2 and ZnO

Batch symbol	SiO_2	Al_2O_3	Fe_2O_3	TiO_2	CaO	MgO	K_2O	Na_2O	P_2O_5	MnO	So_3	Doping additives			Total flux oxides
												CuO	MnO_2	ZnO	
R	59.25	28.90	3.27	1.1	0.50	0.37	2.44	3.61	0.13	0.13	0.36	-	-	-	11.55
RCu2	59.25	28.90	3.27	1.1	0.50	0.37	2.44	3.61	0.13	0.13	0.36	1.94	-	-	13.49
RCu3	59.25	28.90	3.27	1.1	0.50	0.37	2.44	3.61	0.13	0.13	0.36	2.91	-	-	14.46
RCu5	59.25	28.90	3.27	1.1	0.50	0.37	2.44	3.61	0.13	0.13	0.36	4.85	-	-	16.40
RMn2	59.25	28.90	3.27	1.1	0.50	0.37	2.44	3.61	0.13	0.13	0.36	-	1.99	-	13.54
RMn3	59.25	28.90	3.27	1.1	0.50	0.37	2.44	3.61	0.13	0.13	0.36	-	2.98	-	14.53
RMn5	59.25	28.90	3.27	1.1	0.50	0.37	2.44	3.61	0.13	0.13	0.36	-	4.97	-	16.52
RZn2	59.25	28.90	3.27	1.1	0.50	0.37	2.44	3.61	0.13	0.13	0.36	-	-	1.98	13.53
RZn3	59.25	28.90	3.27	1.1	0.50	0.37	2.44	3.61	0.13	0.13	0.36	-	-	2.97	14.52
RZn5	59.25	28.90	3.27	1.1	0.50	0.37	2.44	3.61	0.13	0.13	0.36	-	-	4.95	16.50

RESULTS AND DISCUSSION

The physical properties in terms of linear shrinkage, bulk density, apparent porosity and apparent porosity of different mixes fired between 1000 to 1150°C are shown in Figs. (2, 3 & 4).

The base sample (R sample) fired at 1100°C for 1h, shows linear shrinkage value of 8.50%, bulk density value of 2.58 g/cm^3, water absorption value of `0.05 and apparent porosity value of 0.13%. The bulk density of R sample increased with increasing the firing temperature up to 1100^{o}C, may be due to the crystallization of primary mullite. The water absorption and apparent porosity decreased because of the effect of developed liquid phase in closing the open pore structure. The liquid phase was formed from the melting of Um Risha quartz alkali feldspar syenite and increased with the increasing the firing temperature **Iqbal, (2008).**

RCu2, RCu3 and RCu5 bodies fired at 1050, 1050 and 1025°C for 1h show linear shrinkage values of 7.90, 7.41 and 7.41%, as well as giving bulk density values of 2.60, 2.58 and 2.57 g/cm^3, respectively. Additionally, their apparent porosity and water absorption were zero % as shown in Fig. 2(A, B, C & D) and Table (4).

RMn2, RMn3 and RMn5 bodies fired at 1075, 1075 and 1050°C for 1h, show linear shrinkage values of 7.65 ,7.04 and 7.41%, and giving bulk density values of 2.56, 2.53 and 2.59 g/cm^3, respectively. As well as apparent porosity and water absorption for RMn2, RMn3 bodies were zero and for RMn5 body were 0.15 and 0.39 %, respectively as shown in Fig. 3(A, B, C & D) and Table (4).

RZn2, RZn3 and RZn5 bodies fired at 1100°C for 1h, show linear shrinkage value of 7.65, 7.76 and 7.64% and giving bulk density values of 2.60, 2.60 and 2.61 g/cm^3 also show apparent porosity value of 0.26, 0.39 and 0.13 % and show water absorption value of 0.10, 0.15 and 0.05 %, respectively as shown in Fig. 4 (A, B, C & D) and Table (4).

The addition of CuO to R sample reduced the maturing temperature by about 50°C for RCu2 and RCu3 bodies and by about 75°C for the body RCu5. The addition of MnO_2 to R sample reduced the maturing temperature by about 25°C for the samples RMn2 and RMn3 and by about 50°C for RMn5 sample. The addition of 2, 3 and 5 weight % ZnO to R sample did not cause any change in the maturing temperature of RZn2, RZn3 and RZn5 bodies. The addition of CuO, MnO_2 and ZnO to the base sample (R sample) favoured the crystallization of copper aluminate, manganese aluminate and zinc aluminate phases, respectively that improved the densification of the ceramic bodies produced. The bulk density of the

samples doped with ZnO increased when fired at 1100°C. The results agreed with **Sadek et al. (2023)** who reported that the bulk density of TiO_2–$ZnAl_2O_4$ spinel ceramic bodies increase with increase the firing temperature. The effect of Um Risha quartz alkali feldspar syenite containing a mixture of fluxing oxides (11.55 – 16.50 %) such as CaO, Fe_2O_3, Na_2O and K_2O beside of the added CuO, MnO_2 and ZnO lead to the development of a considerable amount of low viscosity glassy phase which caused a reduce the amount of porosity. **Harms, (1978); Abdel Aziz et al. (2010) and Abdel Aziz et al. (2015)** also reported similar behaviour of alkaline earth oxides in closed the open pores in a porcelain body.

Table (4): Physical properties of the vitrified R sample as pure and doped with CuO, MnO_2 and ZnO

Sample symbol	Maturing Temperatures (°C/1h)	Linear Shrinkage (%)	Bulk density (g/cm^3)	Water absorption (%)	Apparent porosity (%)
R	1100	8.50	2.58	`0.05	0.13
RCu2	1050	7.90	2.60	0	0
RCu3	1050	7.41	2.58	0	0
RCu5	1025	7.41	2.57	0	0
RMn2	1075	7.65	2.56	0	0
RMn3	1075	7.04	2.53	0	0
RMn5	1050	7.41	2.59	0.15	0.39
RZn2	1100	7.65	2.60	0.10	0.26
RZn3	1100	7.76	2.60	0.15	0.39
RZn5	1100	7.64	2.61	0.05	0.13

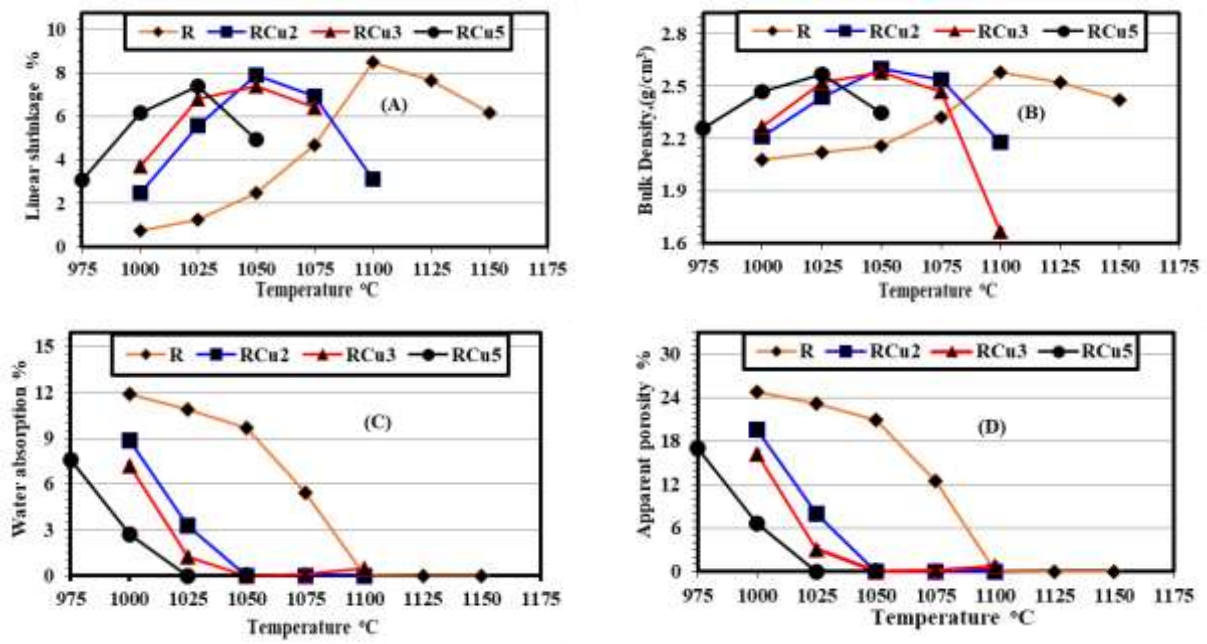

Fig. (2): Physical properties of R sample as pure and doped with 2, 3 and 5 weight % CuO at different sintered temperatures. (A) linear shrinkage, (B) Bulk density, (C)Water absorption, (D)Apparent porosity.

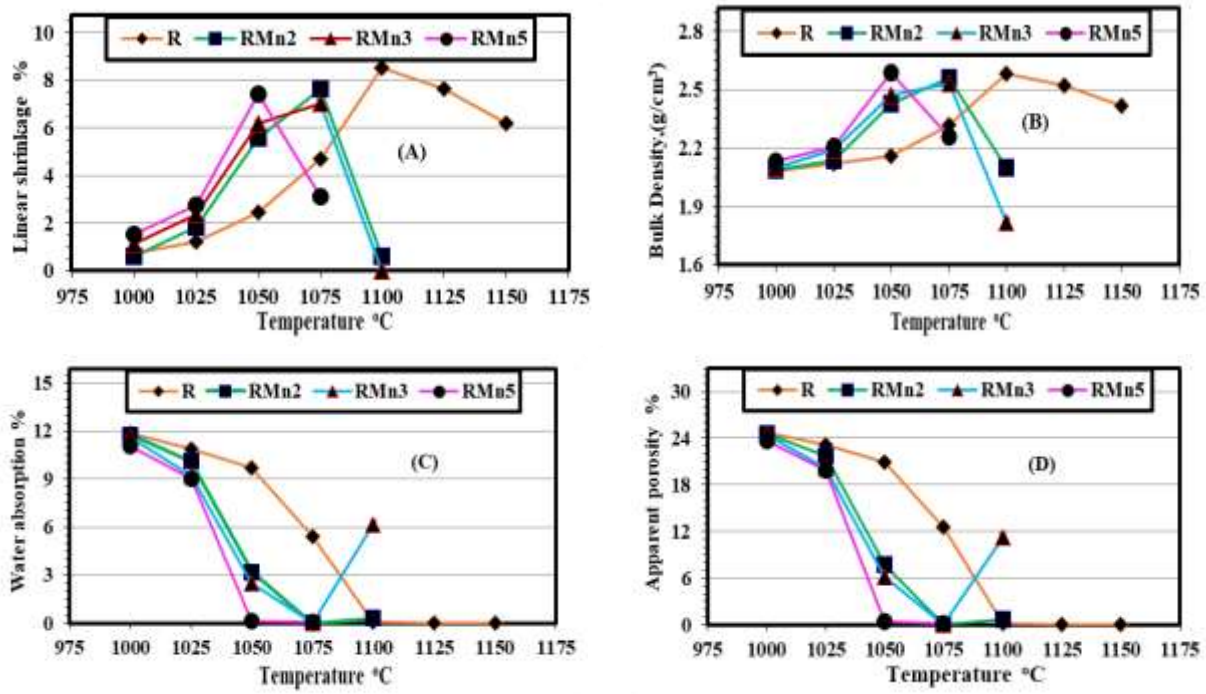

Fig. (3): Physical properties of R sample as pure and doped with 2, 3 and 5 weight % MnO_2 at different sintered temperatures. (A) linear shrinkage, (B) Bulk density, (C)Water absorption, (D)Apparent porosity.

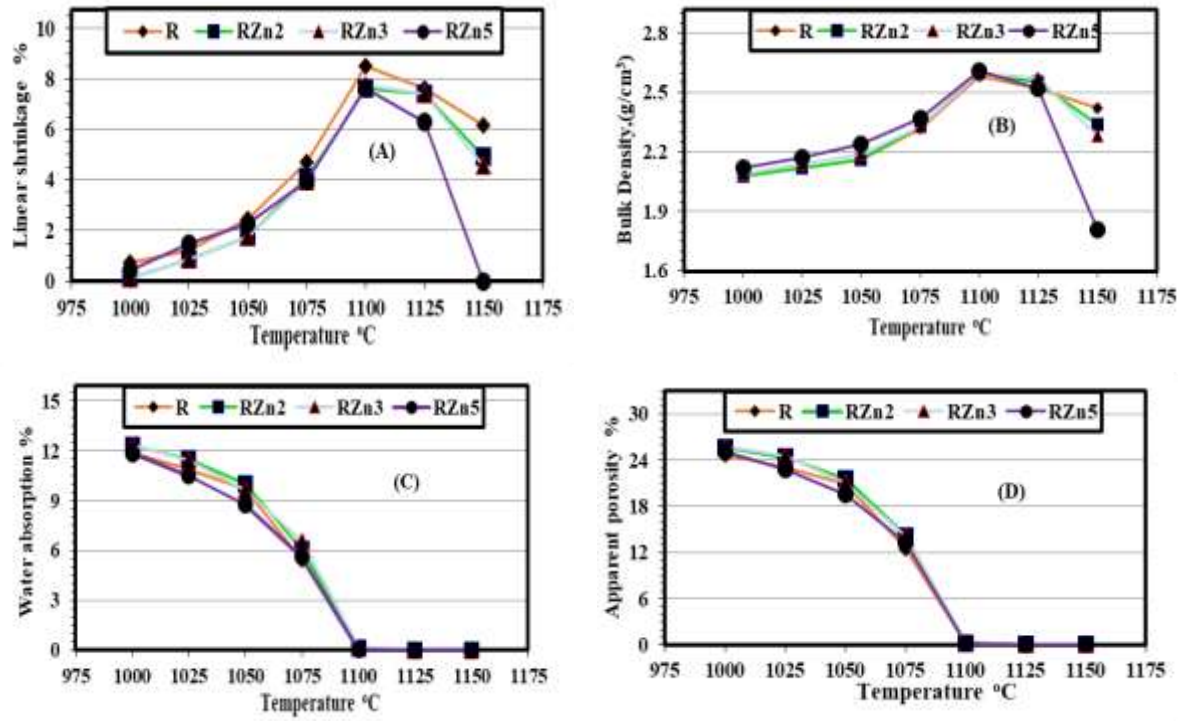

Fig. (4): Physical properties of R sample as pure and doped with 2, 3 and 5 weight % ZnO at different sintered temperatures. (A) linear shrinkage, (B) Bulk density, (C)Water absorption, (D)Apparent porosity.

X- Ray Diffraction analysis (XRD)

XRD analysis of the raw material

Figure (5A) shows the XRD pattern of Um Risha quartz alkali feldspar syenite which composed mainly of microcline, feriferous orthoclase, anorthoclase, albite, aegirine, riebeckite-arfedsonite and quartz. Figure (5B) shows the XRD patter of Abou Seberia clay which composed mainly of kaolinite and quartz. Figure (5C) shows the XRD pattern of alumina which composed mainly of corundum.

XRD analysis of the vitrified R sample as pure and doped with 2, 3 and 5 weight% CuO, MnO_2 and ZnO

The XRD pattern of R sample fired at 1100°C for 1h showed development of crystalline phases as quartz at 2θ 26.64, corundum at 2θ 35.15, trace mullite and minor amount of cristobalite at 2θ 21.41 as shown in Fig. (6). The standard peak of mullite phase at 2θ =16.34 was difficult to detect may be due to the volume fraction and extremely small size, this result is agreement with the results which concluded by **Dana et al. (2004); Hojamberdiev et al. (2011) and Abdel Aziz et al. (2015)**. As well as the peak at 2θ =27.49 refers to microcline mineral.

Figure (6A) shows the XRD patterns of RCu2, RCu3 and RCu5 bodies fired at 1050,1050 and 1025°C, respectively. It is clear that the addition of CuO favoured the crystallization of spinel phase (copper aluminate) $CuAl_2O_4$ which detected at 2θ 36.87 and may be formed by the interaction between the CuO and Al_2O_3. Figure (6B) shows the XRD patterns of RMn2, RMn3 and RMn5 samples fired at 1075,1075 and 1050 °C, respectively. It is clear that the addition of MnO_2 favoured the crystallization of manganese aluminate phase Mn_2AlO_4 which detected at 2θ 35.52, and may be formed by the interaction between the MnO_2 and Al_2O_3. Figure (6C) shows the XRD patterns for RZn2, RZn3 and RZn5 samples fired at 1100°C. It is clear that the addition of ZnO favoured the crystallization of gahnite phase (Zinc aluminate) $ZnAl_2O_4$ which detected at 2θ =36.77 and may be developed by the interaction between ZnO and Al_2O_3.The intensity of peaks for copper aluminate, manganese aluminate and zinc aluminate phase increased with increasing CuO, MnO_2 and ZnO addition, respectively and they were corresponding to decrease in the intensity of peaks related to corundum and mullite as shown in Fig. 6(A, B & C). Um Risha quartz alkali feldspar syenite favoured the dissolution of primary mullite formed from clay in glassy phase rich in silica**.** The presence of CaO and Fe_2O_3 caused the conversion of free quartz into cristobalite. The result is compatible with the results that were

reported by **lee et al. (2005); Abdel Aziz et al. (2010); El-Mehalawy et al. (2018) and Sadek et al. (2023).**

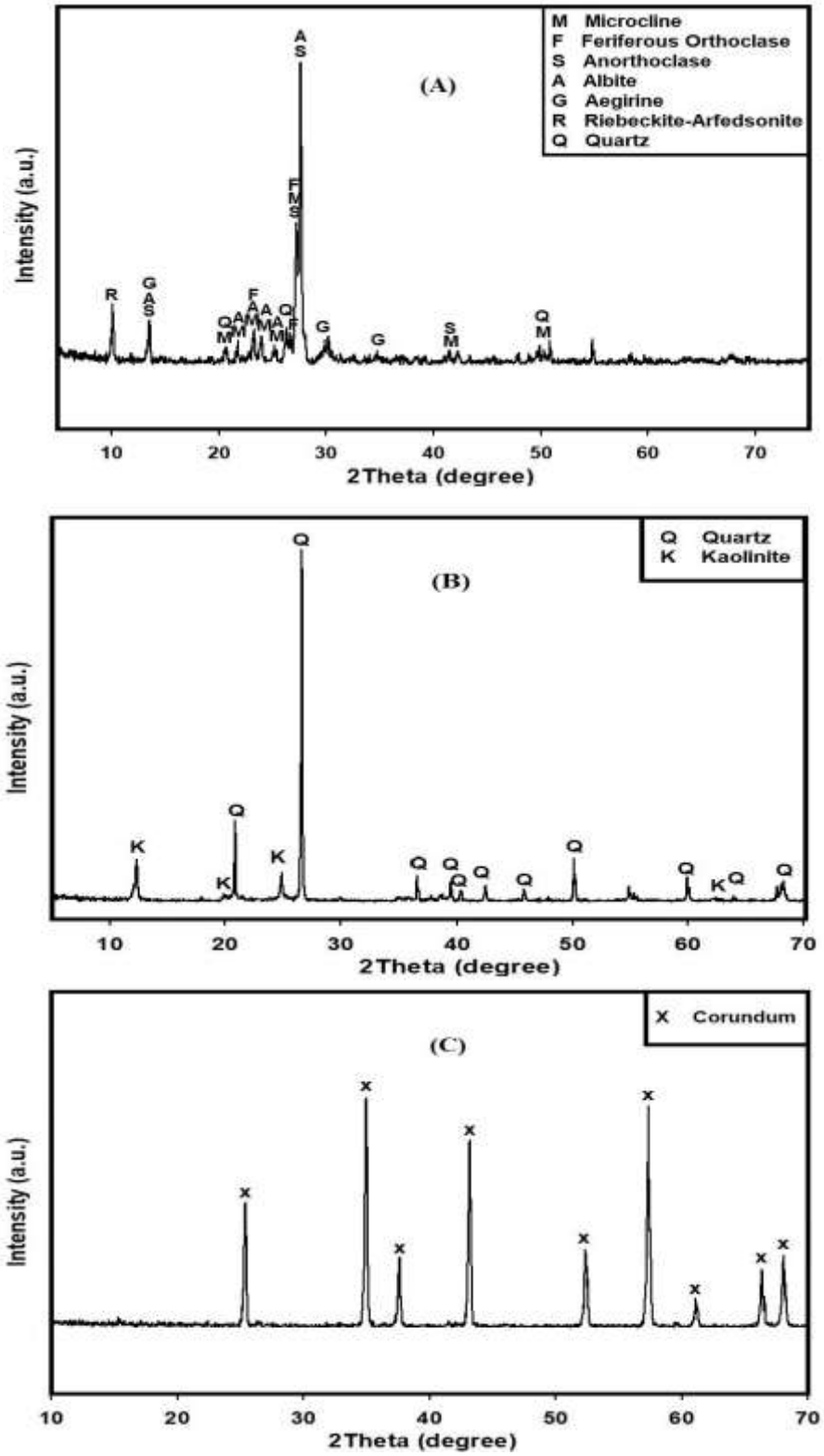

Fig. (5): XRD patterns of (A) Um Risha quartz alkali feldspar syenite, (B) Abou Seberia clay and (C) Alumina.

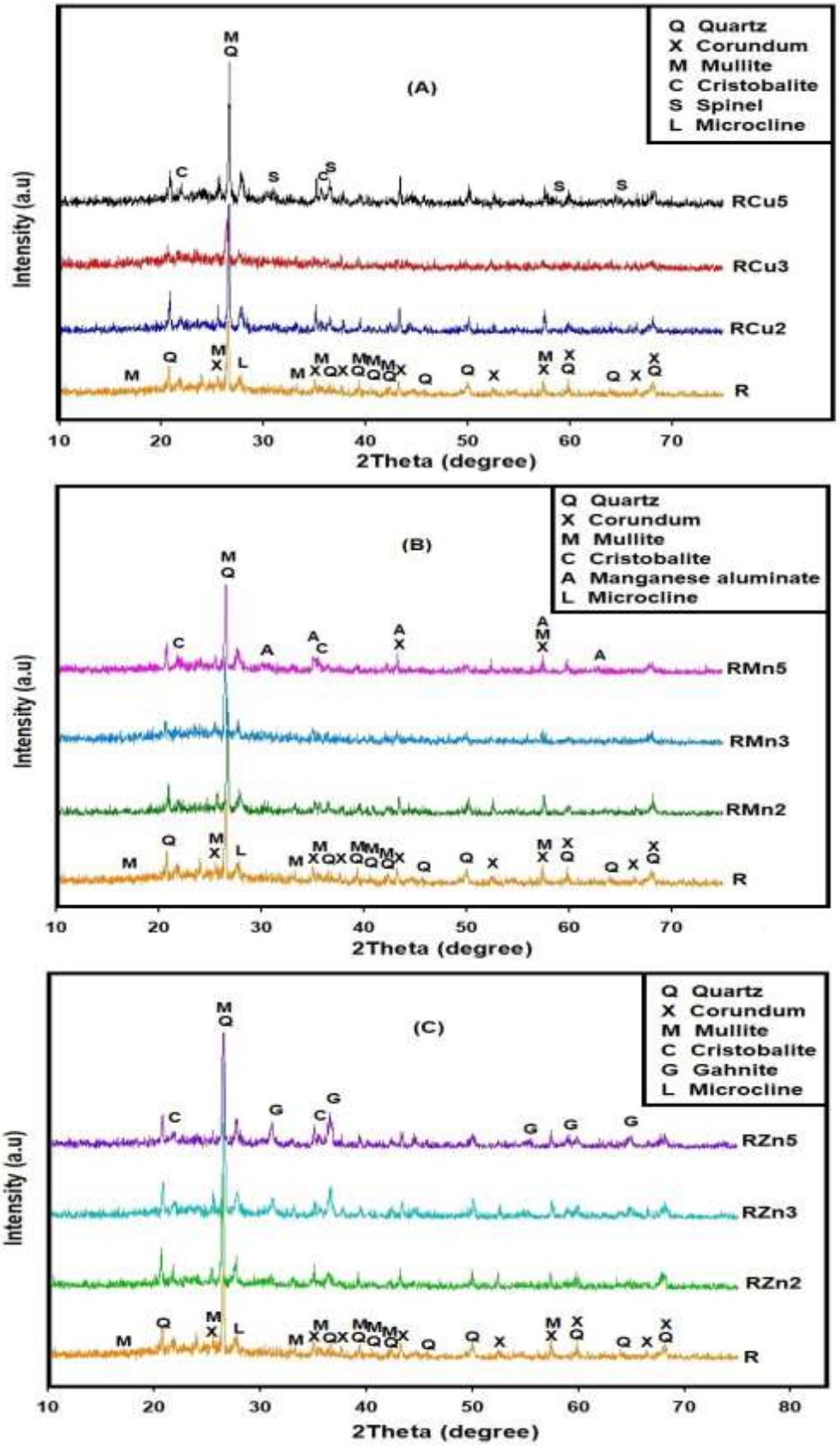

Fig. (6): XRD patterns of the vitrified R sample as pure and doped with 2, 3 and 5 weight % (A) CuO, (B) MnO_2 and (C) ZnO.

Microstructure

Scanning electron microscope (SEM) examine the morphology of different phases as shown in Fig. 7(A, B, C & D)**.** Scanning micrograph for R sample fired at 1100^{o}C shows a several interfering different size and morphology of crystalline phases immersed in a glassy matrix with dense and very low porosity textures. Overall microstructure of vitrified R sample shows the presence of quartz grains, euhedral prismatic alumina crystal and scattered alumina grains. Very small primary mullite crystals grown beside or near the edges of the quartz grains as well as cristobalite grains almost uniformly distributed in glassy matrix as shown in Fig. (7A). The small mullite crystals were possibly crystallized from kaolinite relict. Some of quartz phase seems to be converted to cristobalite phase under the effect of Fe_2O_3 and CaO **(Abdel Aziz et al., 2015).**

The SEM of RCu5, RMn2 and RZn5 body fired at 1025, 1050 and 1100^{o}C showed the crystallization of copper aluminate, manganese aluminate and zinc aluminate phase, respectively occurring in Rosita shape. Additionally interfering of crystalline phases of quartz, corundum, traces of primary mullite and minor amount of cristobalite grains. The phases under consideration immersed in the glassy matrix as shown in Fig.7 (B, C & D).

EDX analysis for the vitrified R, RCu5, RMn2 and RZn5 bodies was performed to confirm the formation of quartz, corundum, mullite, cristobalite phases. Additionally, confirm the crystallization of copper aluminate in RCu5 body, manganese aluminate RMn5 body and zinc aluminate in RZnO as shown in Fig. 8(A, B, C & D). These results agreed with the XRD patterns as seen in Fig. 6 (A, B, C & D).

Electrical properties

The electric properties as dielectric constant, dielectric loss and ac resistivity (ρ) of R sample as pure and doped with 2, 3 & 5 weight % CuO, MnO_2 and ZnO, are represented in Figs. 9(A, B & C), 10(A, B & C) and 11(A, B & C), depending on the rise in the frequency value from 200 Hz up to 50 KHz at the room temperature.

Dielectric properties for the base sample R fired at 1100^{o}C for 1h, depending on the rise in the frequency value from 200 Hz up to 50 KHz at the room temperature showed decreasing in the dielectric constant from 3160.62 to 200.002 and decreasing in dielectric loss from 1.654 to 0.279. As well as the resistivity decreased from 445.304 to 4.477 Ω.m as shown in Fig. 9(A, B & C). Dielectric properties of RCu2, RCu3 and RCu5 bodies fired at 1050, 1050 and

1025^{o}C for 1h gave dielectric constant values of 3563, 3883.14 and 3522.24 at the frequency 200 Hz, and gave values of 217.14, 216.207 and 237.585 at the frequency 50 KHz. The dielectric loss gave values of 1.683, 1.994 and 1.934 at frequency 200 Hz and gave values of 0.329, 0.309 and 0.319 at frequency 50 KHz. The resistivity gave values of 415.13, 433.548 and 457.712 Ω.m at frequency 200 Hz,and gave values of 4.848 ,4.59 and 4.382 Ω.m at frequency 50 KHz, respectively as shown in Fig. 9(A, B & C).

Dielectric properties RMn2, RMn3 and RMn5 bodies fired at 1075, 1075 and 1050^{o}C for 1h, gave dielectric constant values of 4679.1, 4307.43 and 4261.32 at frequency 200 Hz, and gave values of 214.57, 216.333 and 215.668 at the frequency 50 KHz. The dielectric loss gave values of 2.22, 1.824 & 1.97 at 200 Hz and gave values of 0.338, 0.349 and 0.349 at frequency 50 KHz. The resistivity gave values of 403, 341.252 and 373.949 Ω.m at frequency 200 Hz, and gave values of 5.041, 5.085 and 5.182 Ω.m at frequency 50 KHz, respectively as shown in Fig. 10(A, B & C). Dielectric properties of RZn2, RZn3 and RZn5 bodies fired at 1100^{o}C for 1h, gave dielectric constant values of 4512.9, 4017.54 and 3185.13 at the frequency 200 Hz, and gave values of 227.71, 218.204 and 218.854 at the frequency 50 KHz. The dielectric loss of the RZn2, RZn3 and RZn5 bodies gave values of 2.089, 2.209 and 1.856 at 200 Hz and gave values of 0.359, 0.336 and 0.344 at frequency 50 KHz. The resistivity gave values of 373.38, 426.119 and 460.483 Ω.m at frequency 200 Hz and gave values of 5.014, 4.943 and 5.096 Ω.m at frequency 50 KHz, respectively as shown in Fig. 11(A, B & C).

XRD of the samples showed different crystalline phase that immersed in glassy phase as shown in Fig. 6(A, B & C) and SEM 7(A, B, C & D). **Moulson and Herbert, (2003)** reported that the high values in the permittivity for the samples may be due to the accumulation of the charges at the internal boundaries of these phases. Um Risha quartz alkali feldspar syenite developed a considerable amount of low viscosity glassy phase in all the vitrified samples. As a result, mobility of dipoles could be increased leads to improve the dielectric constant of the all bodies. Charge carriers (ions, electrons and holes) and electrical dipole moments move easily in glassy phases than crystalline phase causing the increase of polarization so the dielectric constant increased. The high dielectric constant for the samples doped with CuO, MnO_2 and ZnO corresponding to the low resistivity.

The increasing in the dielectric constant of the sample doped with 2 weight %

CuO, MnO_2 and ZnO compared with R sample. This is attributed to the effect of glassy phase containing Cu^{+2}, Mn^{4+} and Zn^{+2} ions which they have a conductive property **liu et al.(2011) and Valladares et al. (2012)**. The decreasing in the dielectric constant of the samples doped with 5 weight % CuO, MnO_2 & ZnO attributed to the crystallization of copper aluminate, manganese aluminate and zinc aluminate phase which become predominant that resist and cause difficulty in the movement of the charge carries and led to decrease the internal polarization and decrease the dielectric constant and increase the insulating properties of the sample. The result is consistent with the findings of **Sallam et al. (2001**) who found that gahnite phase increased in the volume resistivity. Additionally, it aligns with the results obtained by **Abdel Aziz et al. (2010)**, who found that the crystallization of gahnite phase increased the insulation properties.

The prepared sample at low frequency showed the maximum dielectric constant, this is attributed to the increase of the mobility of charge carrier leading to the increase of the polarization and so the dielectric permittivity. At high frequency the charge carrier mobility cannot follow the high frequency changes and it lags behind the frequency of the external electric field leading to the decrease of polarization and dielectric constant.

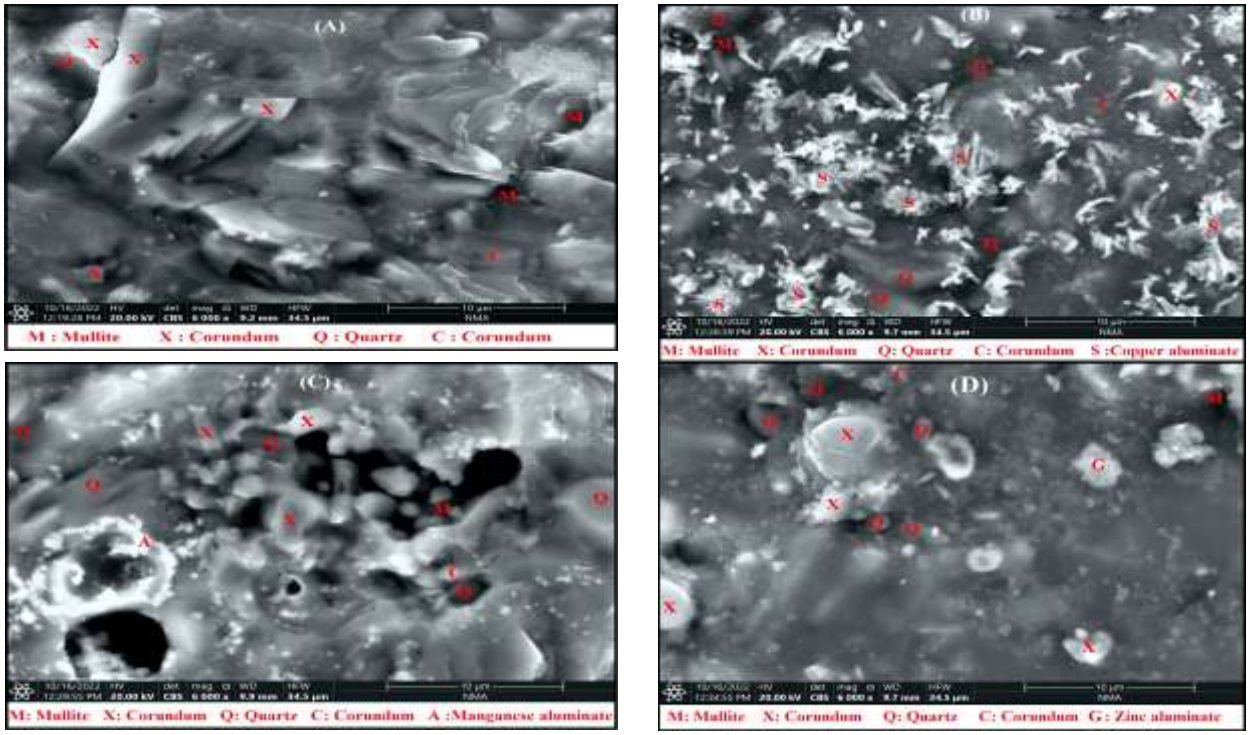

Fig. (7): SEM of (A) R sample sintered at 1100 ^{o}C**,** (B) RCu5 sample sintered at 1025 ^{o}C, (C) RMn5 sample sintered at 1050 ^{o}C and (D) RZn5 sample sintered at 1100 ^{o}C.

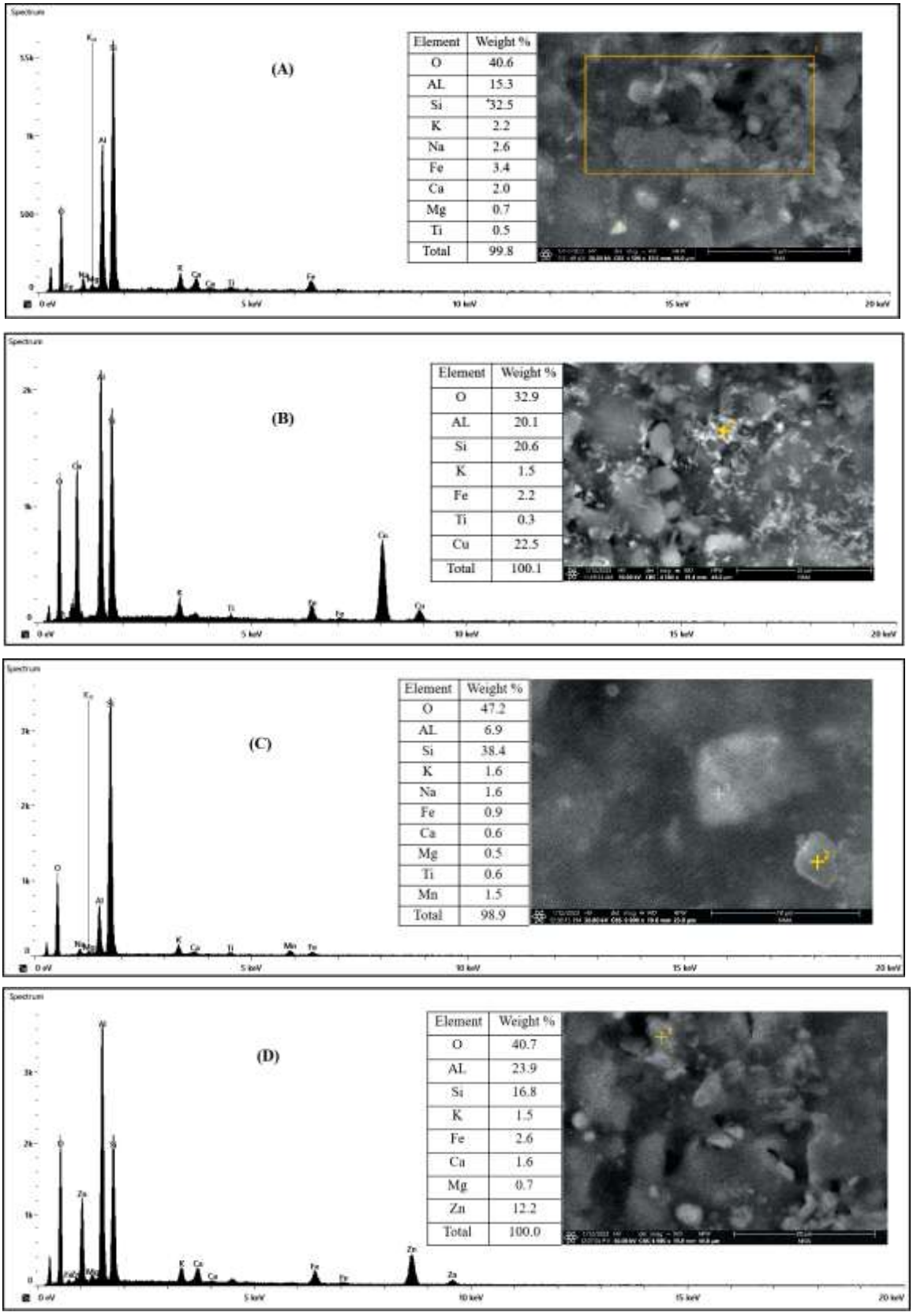

Fig. (8): EDX analysis of (A) R sample sintered at 1100 ^{o}C**,** (B) RCu5 sample sintered at 1025 ^{o}C, (C) RMn5 sample sintered at 1050 ^{o}C and (D) RZn5 sample sintered at 1100 ^{o}C **.**

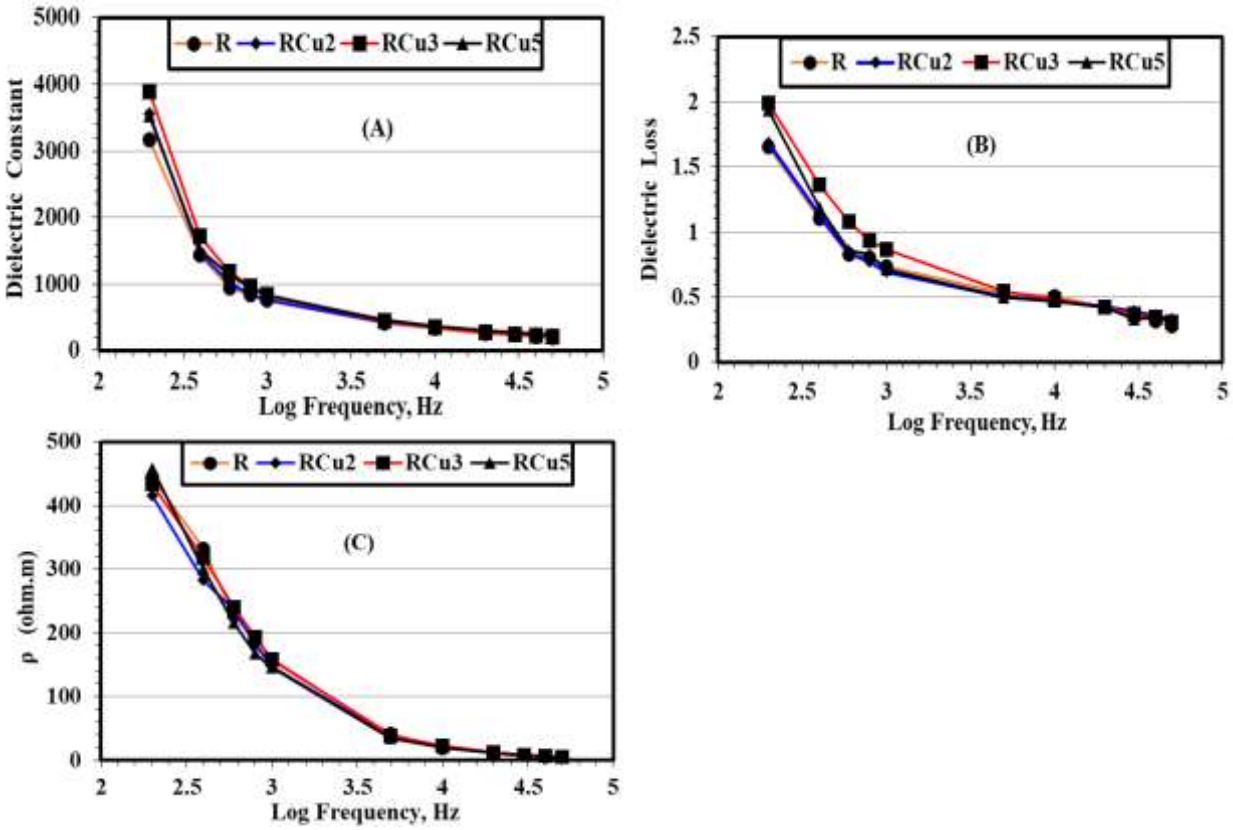

Fig. (9): Electrical properties of the vitrified R sample as pure and doped with 2, 3 and 5 weight % CuO, (A) Dielectric constant, (B) Dielectric loss, (C) Resistivity.

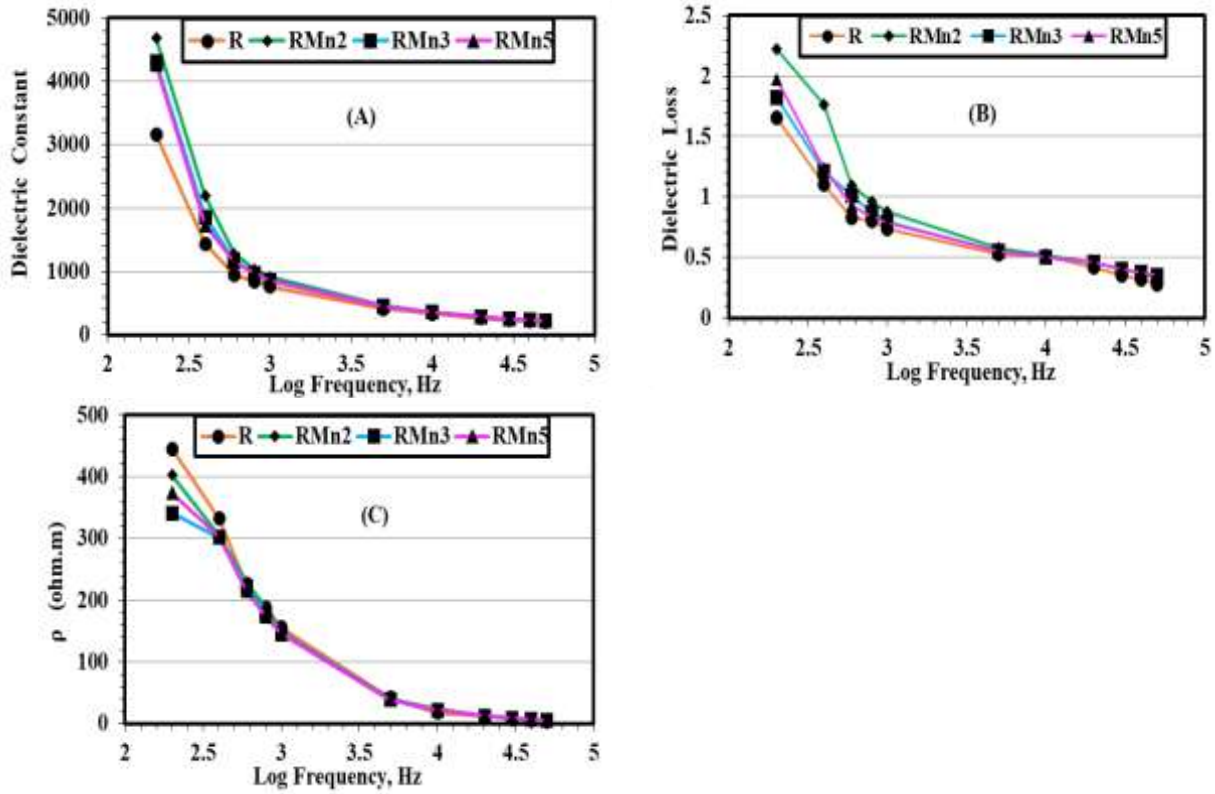

Fig. (10): Electrical properties of the vitrified R sample as pure and doped with 2, 3 and 5 weight % MnO_2, (A) Dielectric constant, (B) Dielectric loss, (C) Resistivity.

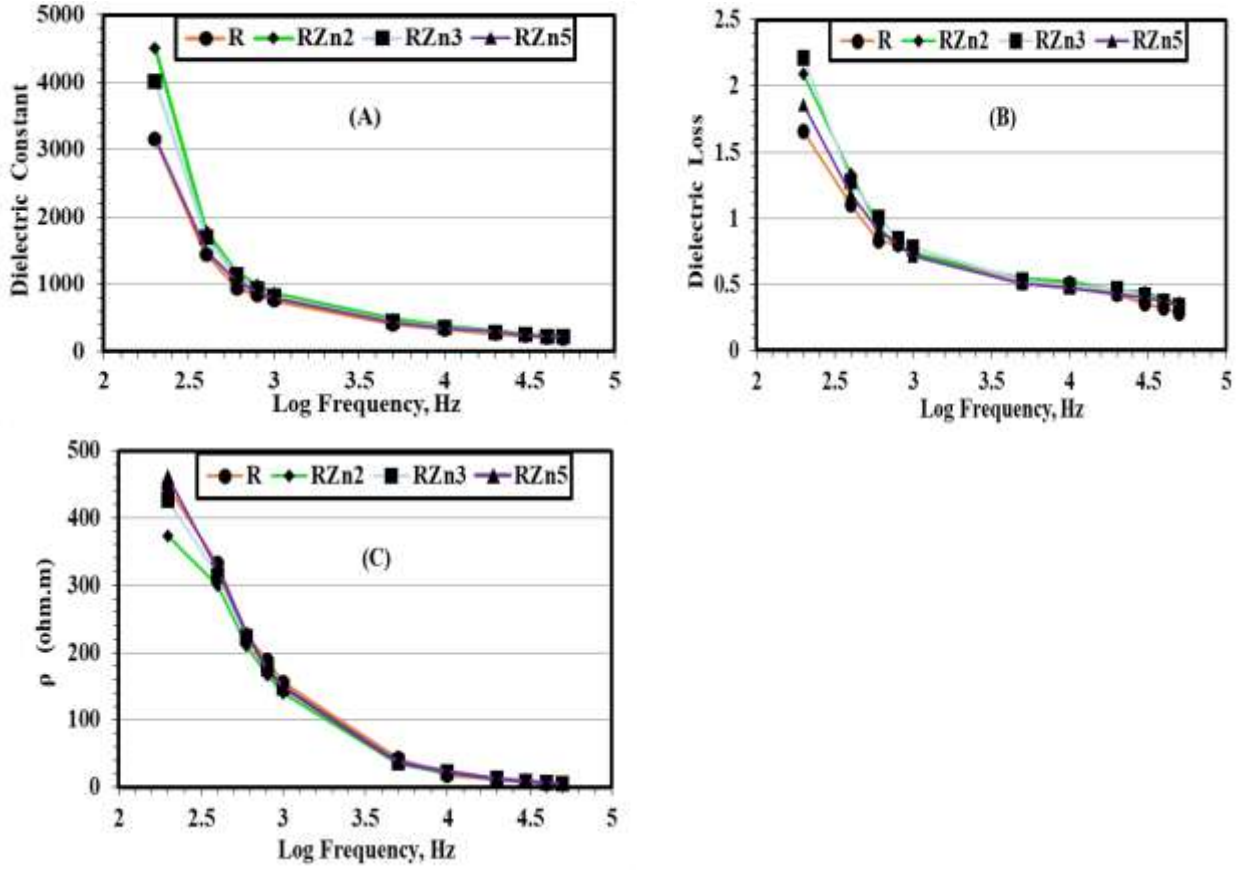

Fig. (11): Electrical properties of the vitrified R sample as pure and doped with 2, 3 and 5 weight % ZnO, (A) Dielectric constant, (B) Dielectric loss, (C) Resistivity.

Conclusion

The addition of the coflux oxides (CuO, MnO_2& ZnO) as doping additives to the pure base sample which composed of 50 Um Risha quartz alkali feldspar syenite, 40 Abou Seberia clay and 10 alumina, weight % resulted in producing ceramic bodies with semiconductor properties which is employed in capacitor fabrication. The other finding is lowering of the maturing temperature by 25 - 75^{o}C in the samples that doped with CuO and MnO_2 which considered an important aim in the purpose of saving energy.

References:

Abdel Aziz, D. A., Mahani R., Ibrahim D. M. and Aly M. H. (2010). physico-electrical properties of ceramic bodies based on nepheline tailing and clay. *Ind. Ceram*., 30: 89-95.

Abdel Aziz, D. A., Aly, M. H., Salem, I. A., Abead, S. A. (2015). Effect of Air Blast Furnace Slag and γ-Alumina Content on Dielectric Properties and Physical Properties of Porcelain Insulators. *Phys. Mat. Chem*., 3: 30-36.

Anonymons, (1975). Annual book of ASTM standards part 17. *Amer. Soc. Test*. Mater.

Burat, F., Kangal, O., Onal, G. (2006). An alternative mineral in the glass and ceramic industry: nepheline syenite. *Miner. Eng.*, 19: 370–371

Dana, K., Das, S. and Das, S.K. (2004). Effect of substitution of fly ash for quartz in triaxial kaolin–quartz–feldspar system, *J. Eur. Ceram. Soc*., 24: 3169-3175.

El-Ramly, M.F., Budanov, V.I., Armanious, L.K., Dereniuk, N.E., (1969b). The three ring complexes of gabal El Kahfa, gabal Nigrub El fogani and gabal El Naga, S. E. Desert of Egypt. *Geol. Surv. Egypt*. , 52: 1– 39.

El-Ramly, M.F., Hussein, A.A., (1982). The alkaline ring complexes of Egypt. *Geol. Surv. Egypt*. Paper no. 63 -16.

El-Ramly, M.F.; Budanov, V.I.; Hussein, A. A., and Dereniuk, N.E., (1970). Ring complexes in the south Eastern Desert of Egypt. In: Studies of some mineral deposits of Egypt, (Osman Moharam et al., Eds.), *Geol. Surv. Egypt*, 181- 194.

El-Mehalawy N., Awaad M., Eliyan T., Abd-Allah M.A., Naga S.M., (2018). Electrical properties of ZnO/alumina nano composites for high voltage transmission line insulator. *J. Mater. Sci. Mater. Electron.* 29(16): 13526–13533.

Harms, W. (1978). Fast firing dinnerware: state-of-art. *Ceram. Ind. Mag*., 110: 20-23.

Hojamberdiev, M., Eminov, A. and Xu. Y. (2011). Utilization of muscovite granite waste in the manufacture of ceramic tiles. *Ceram. In*t., 37: 871-876.

Ibrahim, D.M., Sallam, E.H., Khalil, A.A., Naga, S.M. (1981). Nepheline syenite-talc low temperature vitrified bodies. *Ceram. Int.*, 7: 69–72.

Iqbal, Y. (2008). On The Glassy Phase In Tri-Axial Porcelain Bodies. *J. Pak. Mater. Soc.*, 2(2), 62-71.

Ismail, A. I. M., Elmaghraby, M. S. and Shalaby. B. N. A. (2022). Flux ceramic tiles based on Egyptian trachyte. *Bull. Nat. Res. Cent.*, 46: 226.

Kingery, W.D., Bowen, H.K., Uhlmann, D.R. (1975): Introduction to Ceramics. 2nd ed., Wiley, New York 495.

Lee S.M., Kim S.K., Yoo J.W. and Kim H.T., (2005). Crystallization behavior and mechanical properties of porcelain bodies containing zinc oxide additions. *J. Eur. Ceram. Soc.* 25: 1829-1834.

Liu M, Lin M. C. and Wang, C. (2011). Enhancements of thermal conductivities with Cu, CuO, and carbon nanotube nanofluids and application of MWNT/water nanofluid on a water chiller system. *Nanoscale Res. Let.*, 6: 297.

Milankovic A.M., Santic A., Gajovic A., Day D.E. (2001). Electrical properties of sodium phosphate glasses containing Al_2O_3 and/or Fe_2O_3. *J. Non-Crys. Solids*, 296: 57-64.

Moulson A.J. and Herbert J.M. (2003). Electro-ceramics: Materials, Properties and Applications, 2nd ed., John Wiley & Sons, Ltd, Chichester, UK.

Pantshi, B. and Theart, H.F.J. (2008). The Red Syenite of the Pilanesberg Complex: A Potential Raw Material Source for the South African Ceramics and Glass Industry. *South Afr. J. Geol.*, 111: 27-38.

Ryshchenko, M.I., Shchukina, L.P., Fedorenko, E.Y., Firsov, K.N(2008). Possibility of obtaining ceramogranite using quartz-feldspar raw material from Ukraine. *Glass Ceram*. 65[1–2]: 23–26.

Sadek H. E. H. , Reda A. E., Khattab R. M. and Hessien M. A. (2023). The Role of TiO_2 on $ZnAl_2O_4$ Spinel Prepared by Direct Coagulation Casting Method: Physico-mechanical, Optical,

Structural and Antimicrobial Properties. *J. Inorg. Organomet. Poly. Mater.*, 34: 1350-1368.

Salem, A., Jazayeri, S.H., Rastelli, E., Timellini, G. (2009). Dilatometric study of shrinkage during sintering process for porcelain stoneware body in presence of nepheline syenite. *J Mater. Process Tech.*, 209:1240–1246.

Sallam E.H., El-Didamony H., Abdel Aziz D.A., Naga S.M. (2001). Influence of Zn^{2+} ion addition on properties of aluminous electrical porcelain. Brit. Ceram., 100(4):177-180.

Sindhu S., Ranatharaman M., Thampi P.B., Malini K.A., Kurian P. (2002). *Bull. Mater. Sci*. 25/7, 559.

Valladares L. D. L. S., Salinas D.H., Dominguez A.B., Najarro D.A., Khondaker S.I., Mitrelias T., Barnes C.H.W., Aguiar J.A. and Majima y. (2012). Crystallization and electrical resistivity of Cu_2O and CuO obtained by thermal oxidation of Cu Thin films on SiO_2/Si Substrates. Thin Solid Films. 520: 6368–6374.

الخواص العزليه والتركيب الدقيق للأجسام السيراميكيه المحتويه علي سيانيت أم ريشه والمشوبه بالمصهرات الحفازه

الباحث/ صلاح عبدالغني عبيد[١]، ا.د إبراهيم عبالناجي سالم[١] ،ا.د دعاء عبدالنبي عبدالعزيز[٢]، ا.د محمد متولي أبوعنبر[١]،

ا.د مبارك حساني علي[٣] ، ا.د أسامه محمد حميده[٤] ، د.بسنت إبراهيم سالم[٤]

[١] قسم الجيولوجيا - كلية العلوم - جامعة طنطا
[٢]قسم السيراميك - المركز القومي للبحوث
[٣]معهد الدراسات والبحوث البيئيه - جامعه مدينة السادات
[٤] قسم الفيزياء- كلية العلوم - جامعة طنطا

تقع منطقة ام ريشه في جنوب الصحراء الشرقيه ما بين خطي عرض ٢٣° ١٥/ - ٢٣° ٢٠/ وخطي طول ٣٣° ١٥/ - ٣٣° ٢٠/ . منطقة أم ريشه من المعقدات الحلقيه وتتكون معظمها من صخور الجرانيت والسيانيت .

يتناول هذا البحث دراسة إضافة سيانيت أم ريشه المحتوي علي ٤,٩٨% من أكسيد الحديد وعلي٤,٣٧% من أكسيد البوتاسيوم وعلي ٧,٠٦ % علي أكسيد الصوديوم كماده صهاره لتكوين جسم سيراميكي بخلطه أساسيه تتكون ٥٠% سيانيت أم ريشه، ٤٠% طفلة أبوسبيره،١٠% اكسيد الومنيوم . كما تم إضافة المصهرات الحفازه مثل أكسيد النحاس – ثنائي أكسيد المنجنيز- أكسيد الزنك بنسبة ٢-٥% إلي الخلطه الأساسيه للحصول علي أجسام سيراميكيه ذات الخصائص الطبيعيه والكهربيه المميزه بخصائص أشباه المواصلات التي يمكن استخدامها لعمل المكثفات وذلك بإستخدام سيانيت أم ريشه والأكاسيد المصهره الحفازه المختاره.

لتحقيق الهدف من الدراسه تم إستخدام الطرق المعمليه الأتيه:

١) التحليل الكيميائي للعناصر الشائعه لسيانيت منطقة أم ريشه وطفلة أبوسبيره وأكسيد الالومنيوم وإستخدام الأشعة السينيه لدراسة المعادن الموجوده بالخامات الأوليه المستخدمه في عمل الخلطه الأساسيه.

٢) تجهيز ١٠ خلطات عباره عن الخلطه الأساسيه بدون إضافة أو بإضافة ٢-٥% من المصهارات الحفازه المختاره . تم طحن هذه الخلطات لمدة ساعتين وتجفيفها وكبسها تحت ضغط ٢٣٠ كجم/سم[٢] علي شكل أقراص ذات قطر١٦ مم وسمك ≤ ٤.٨ مم .و تجفيف العينات بعد كبسها في الهواء لمدة ٤٨ ساعه ثم وضعها في مجفف كهربائي عند درجة ١١٠°م لمدة ٢٤ ساعه وتم حرق هذه العينات ما بين ١٠٠٠ الي ١١٥٠°م لمدة ساعة.

٣) دراسة الخواص الفيزيائيه مثل الإنكماش الطولي والكثافه النوعيه وإمتصاص الماء والمساميه الظاهريه للعينات المحروقه عند درجات الحراره المختلفه وذلك لتعيين درجة حرارة النضج. ومن النتائج اتضح أن درجة حرارة ١١٠٠°م هي درجة حرارة النضج للخلطه الأساسيه . أما عند إضافة ٢-٥ % من أكسيد النحاس وثاني أكسيد المنجنيز للخلطه الأساسيه نتج عنه خفض في درجة حرارة النضج بحوالي ٢٥ -٧٥ °م ولم يحدث أي تغير في درجة حرارة النضج عند إضافة أكسيد الزنك.

٤) دراسة الاطوار البللوريه المتكونه في الخلطات المحروقه (١٠ خلطات) عند درجات حرارة النضح بإستخدام الأشعه السينيه. وأوضحت النتائج تكون اطوار بلوريه من الكوارتز والكوراندم مع قليل من معدن موليت والكرستوباليت بالإضافه تواجد معدن الميكروكلين. أما عند إضافة الاكاسيد المصهره الحفازه أدي الي تكوين طور بللوري جديد وهو الاسبنيل بالاضافه الي الاطوار البللويه المذكوره في الخلطه الاساسيه.

٥) إستخدام الميكروسكوب الماسح لتحديد الأطوار المتبلوره للخلطات المحروقه عند درجات درجة حرارة النضج.

٦) تحديد الخصائص الكهربيه مثل ثابت العزل وفاقد العزل والمقاومه النوعيه المقاسه مابين ٢٠٠ – ٥٠٠٠٠ هيرتز في درجة حراره الغرفه للاجسام السيراميكيه عند درجات حرارة النضج . من القياسات الكهربيه تم الحصول علي نتائج متقاربه سواء بإضافه اوبدون إضافة الأكاسيد المصهره الحفازه مع ملاحظة انخفاض ثابت العزل بزياده نسبة إضافة الاكاسيد المصهره من ٢ إلي ٥ % ويعزى ذلك الزيادة في تكون معدن الاسبنيل مع زياده نسبة اضافة الاكاسيد المصهره الحفازه. وهذه النتائج تعزي الي إستخدام هذه الأجسام السيرميكيه محل الدراسه كأشباه مواصلات والتي يمكن الاستفاده في عمل المكثفات.